Ninth International Conference on WWER Fuel Performance, Modelling and Experimental Support, Helena Resort near Burgas, Bulgaria, from 17 to 24 September , 2011.

Total Surface Area change of Uranium Dioxide Fuel in Function of Burn-up and its Impact on Fission Gas Release During Neutron Irradiation for Small, Intermediate and High Burn-up.

Marcin Szuta

Institute of Atomic Energy POLATOM, Otwock-Swierk 05-400, Poland
E-mail: mszuta@cyf.gov.pl

Abstract

In the early published papers it was observed that the fractional fission gas release from the specimen have a tendency to increase with the total surface area of the specimen - a fairy linear relationship was indicated. Moreover it was observed that the increase of total surface area during irradiation occurs in the result of connection the closed porosity with the open porosity what in turn causes the increase of fission gas release. These observations let us surmise that the process of knock-out release is the most significant process of fission gas release since its quantity is proportional to the total surface area. Review of the experiments related to the increase of total surface area in function of burn-up is presented in the paper.

For very high burn-up the process of grain sub-division (polygonization) occurs under condition that the temperature of irradiated fuel lies below the temperature of grain re-crystallization. Simultaneously with the process of polygonization, the increase in local porosity and the decrease in local density in function of burn-up occurs, which leads to the increase of total surface area.

It is suggested that the same processes take place in the transformed fuel as in the original fuel, with the difference that the total surface area is so big that the whole fuel can be treated as that affected by the knock-out process. This leads to explanation of the experimental data that for very high burn-up (>120 MWd/kgU) the concentration of xenon is constant.

An explanation of the grain subdivision process in function of burn-up in the “athermal” rim region in terms of total surface area, initial grain size and knock-out release is undertaken.

Correlation of the threshold burn-up, the local fission gas concentration, local total surface area, initial and local grain size and burn-up in the rim region is expected.

Keywords: total surface area, grain subdivision, rim region, fission gas, knock-out release.

1. Introduction.

Light water reactors (LWR) use uranium dioxide (UO_2) fuel, or a mixture of uranium and plutonium dioxide (MOX) fuel. The fuel is prepared in the form of pellets piled-up in a metallic cladding material. The fuel pellets are manufactured by sintering UO_2 powder compacts for a few hours at 1600–1700 °C under a controlled atmosphere. Sintering is terminated at a density from 93% and 97% of the theoretical maximum. The pellets contain from 7% to 3% of residual pores. Incorporation of some porosity in the fuel is desirable for long burn-up operation, in order to trap the fission gas products, and to accommodate the swelling. On the other hand, this initial porosity introduces secondary effects on all the UO_2 physical properties, e.g., thermal conductivity, creep and strength, and elastic constant. The selection of UO_2 over other potential fuel materials for light water reactors, is based on its excellent combination of chemical stability, especially to water reactor coolants and its compatibility with the potential cladding materials, such as stainless steel and zircaloy. Good irradiation stability and high retention capability for the fission products, thanks to a rather open crystal lattice (face-centered cubic lattice structure of the CaF_2-type). Also, very high melting point (2865±15 °C), with no phase transformation occurs up to this melting point, and a large range of non-stoichiometry, extending from about $UO_{1.65}$ to $UO_{2.25}$ at ~2427 °C.

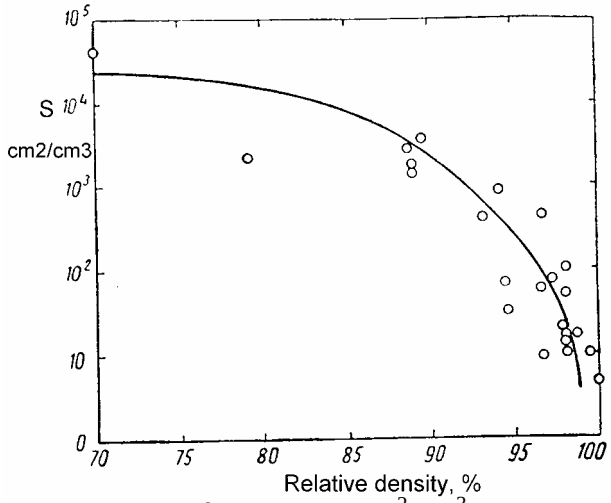

Fig. 1.Total surface area S [cm^2/cm^3] versus relative density [%] of sintered UO_2 [1].

Total surface area of sintered UO_2 powder compacts in function of relative density was measured [1] as an important feature of the fuel. In figure 1 is presented dependence of total surface area on relative density. The dependence was obtained according to the data published in [2] and [3].

In the early work [4] published in 1965 the author observed that the fractions of ^{133}Xe released from the specimen and evolved in the void space of the capsule have a tendency to increase with the BET-surface of the specimen.

The fraction of ^{133}Xe released is plotted against BET-surface area as shown in Fig. 2.

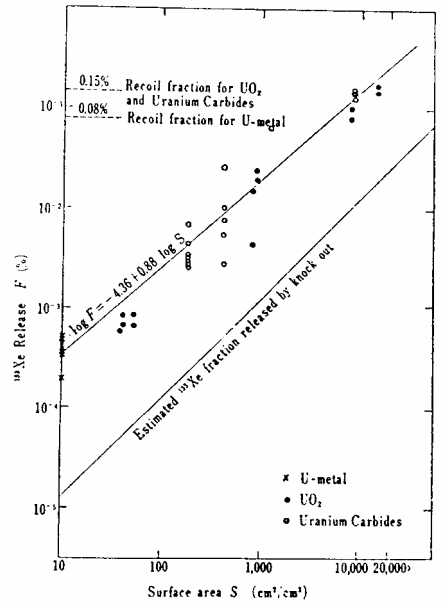

Fig. 2. The fraction of ^{133}Xe released the void space of the capsule [4].

In this logarithmic representation, a fairy linear relationship is indicated between the fractional release of ^{133}Xe and BET-surface area. An equation fitting this line can be drawn by least square method using the averages of several measurements for each surface area. The equation thus determined is:

$$\text{Log } F = -4.36 + 0.88 \log S, \qquad (1)$$

where F- the fraction of ^{133}Xe released produced by fission in the specimen (%), S – BET-surface area (cm^2/cm^3).

2. Total surface area change of uranium dioxide fuel for small and intermediate burn-up.

Uranium dioxide irradiated to a fluency of greater than 10^{19} fissions/cm^3 (burn-up about 0.4 MWd/kg UO_2 which is obtained after several days of exploitation) is found to immobilize practically 99.9 % of generated fission gases.

It is assumed that the fission gas immobilization is due to radiation induced chemical activity and the generation of fission gas bubbles in the solid. Only small part of the immobilized fission gas is in the generated bubbles.

After crossing a certain limit of fission fluency (burn-up) in uranium dioxide an approximately constant high concentration of intra-granular fission-gas bubbles independent of both irradiation temperature and burn-up is always found [5].

The fission gas can escape from the fuel through channels which are formed instantaneously, between the bubble traps and the fuel surface., by the fission products [6]. The hypothesis is advanced that this is the only significant method of release from the bubble traps. This follows from comparing Nelson's conclusion [7] (that the geometrical surface area of the specimen is important when UO_2 molecules are knocked-out from the fuel surface) and the experimental data given in refs. [4, 8, 9,] (showing that the quantity of the fission gas released during irradiation depends on the total surface are of the specimen).

The knock-out process affects the UO_2 fuel surface layer to a depth of not more than 10

μm (the maximum fission product range in UO_2 fuel [1]). The knock-out pertaining to UO_2 molecules and, together with them, to the dissolved fission gas atoms, which mostly have sufficient energy to re-enter the specimen, should be distinguished from that of fission gas atoms which follow the fission fragment out of a bubble.

It has been assumed, in accordance with the data given in refs [4,9,10,11] that the rate of release of fission gas is proportional to the knock-out rate and concentration of gas trapped in the bubbles. It may further be assumed that not all the gas trapped in the bubble is released in a single knock-out depends slightly on the fuel temperature. Nevertheless, the local temperature due to the thermal spike is decisive for the fission gas release process.

Fig. 3. presents [12] the ratio of total surface area (S) to volume (V) for two different specimens plotted against burn-up.

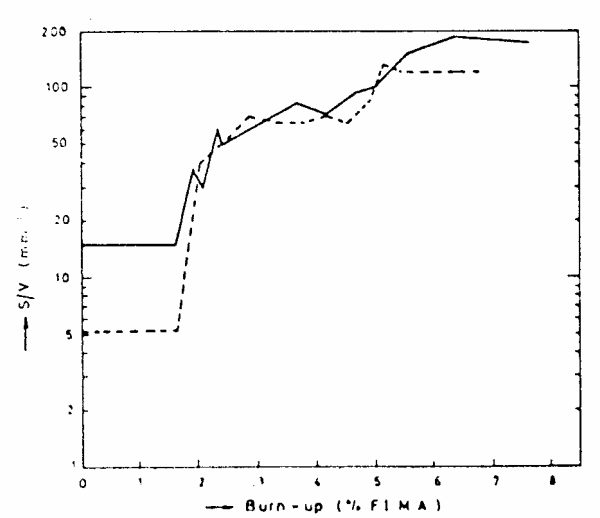

Fig. 3. (S/V) plotted against burn-up for two different specimens [12].

Another example of the ratio of total surface area to volume ratio is the Fig. 4 [13] for the standard 6 μm grain size fuel investigated in the gas flow rig IFA-504 of OECD Halden Reactor Project.

The burn-up dependence of the surface to volume ratio (S/V) of the fuel continues to show no difference between different grain size fuel. After a second porosity inter-linkage period, S/V in rods 1, 2 and 4 has decreased in response to re-sintering processes. In contrast, re-sintering of the doped fuel in rod 3 is proving to be a slow process.

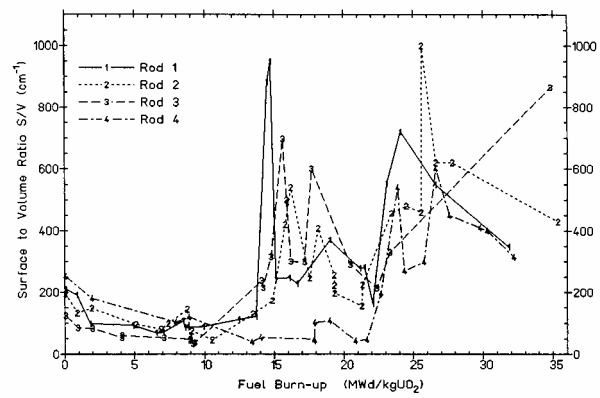

Fig. 4. Surface to volume ratio plotted as a function of burn-up [13]

Assuming the above assumptions and the experimental data underlining the inter-linkage process depending on burn-up we can write that the fission gas release during irradiation according to the defect trap model is equal:

$$R = g_2 f M_{tr} \frac{(S\ x\ r)}{V} \tag{2}$$

$$S = S_0 + S_1 \left(1 - \exp\left(-\frac{Bu - B_0}{\tau}\right)\right) \tag{3}$$

where

f - fission rate, r - fission product range, B - burn-up, M_{tr} - concentration of gas atoms in the bubbles, S - total surface area, V – sample volume and g_2, S_0, S_1, B_0, τ - constants.

3. Total surface area change of uranium dioxide fuel for very high burn-up.

In order to find an answer what causes the increase of total surface for very high burn-up we have to look carefully at the experimental data available in the open literature which concern the grain subdivision process.

The local xenon concentrations in the UO_2 matrix measured by EPMA as a function of the local burn-up is presented in Fig. 5 [14]. Only xenon concentrations not affected by thermal fission gas release are considered. Included are data from different reactors (BWR, PWR, Belgim BR-3 reactor) fuel from different vendors, fuel of different design and xenon measurements from different sources (ITU and HBEP). These differences explain most of the scatter of the Xe concentrations [14]. Some trends are clearly visible:

- At about 1 wt % which corresponds to a burn-up of 60 – 75 MWd/kgU the xenon concentrations deviates from the generated Xe concentration.
- A more or less linear behaviour of the Xe concentration up to the threshold burn-up of about 60 – 75 MWd/kgU is followed by a sharp decrease of Xe in the matrix, which denotes the formation of the nanostructure.
- At high burn-up above 120 MWd/kgU the Xe concentration does not fall below a concentration of approximately 0.25 wt % and approaches an equilibrium between generated and released Xe.

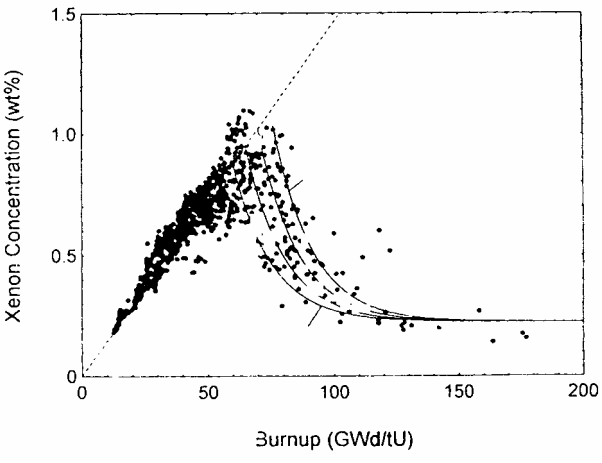

Fig. 5. Local xenon concentration as a function of the local burn-up; the threshold burnup was varied between 60 and 75 GWD/tU.[14]

The large-grained pellets show remarkable resistance to the rim structure formation [15](see Fig. 6) The xenon concentration in the BLH-64-43 type fuel of large grain fuel (grain size equal to 78 μm) continues to climb with burn-up above 75 GWd/tU confirming that the high burn-up structure had not formed to the usual extent in this large grain fuel.

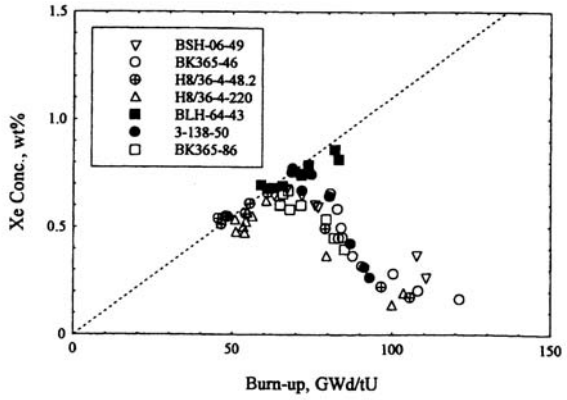

Fig. 6. Local concentration of xenon measured by EPMA in the outer region of the fuel [15].

The xenon concentration falls beyond 60 – 75 GWd/tU due to formation of the high burn-up structure. The dashed line represents the predicted relationship without release based on a hypothetical fission yield of 0.21. Note that the xenon concentration in the fuel BLH-64-43 continues to climb with burn-up above 75 GWd/tU indicating the absence of the high burn-up structure. Only the fuel noted BLH-64-43 had an abnormally large grain size of 78 μm obtained by the addition of 0.46 wt% Nb_2O_2 in comparison of the other fuel (BSH-06-49, BK365-46, H8/36-4-42.2, H8/36-4-220, 3-138-50, BK365-86) used in the experiment [15].

We can infer from the Fig. 6 that the big scatter of the xenon concentrations in fig. 5 after crossing the first threshold burn-up is caused by different grain sized fuel from different reactors. This conclusion is supported by the smooth shape of the curve of xenon concentration change with burn-up for the equal size grained fuels presented in Fig. 6.

The effect of large grain structure on the rim structure formation was studied by Une et al. [16]. Besides the standard grain size pellet, several types of improved pellets were fabricated and loaded in fuel rods. Two types of undoped and alumino-silicate doped large grained pellets were used. The three types of pellets are given in Table 1. The density for all the pellets was high at 97 – 98 % TD, and the grain size was 9 – 12 μm for the standard pellet, 51 – 63 μm for the undoped large grained pellet and a wide range of 37 – 58 μm for the synthetic alumino-silicate doped pellet, depending on the additive concentration of 0.025 – 0.25 wt%.

Table 1. Grain size and density of UO_2 fuel pellets.

Pellet type	Grain size (μm)	Density (% TD)
Standard grain	9 – 12	96.8 – 97.2
Large-grain	51 – 63	96.4 – 96.9
Doped large-grain	37 – 58	97.1 – 97.8

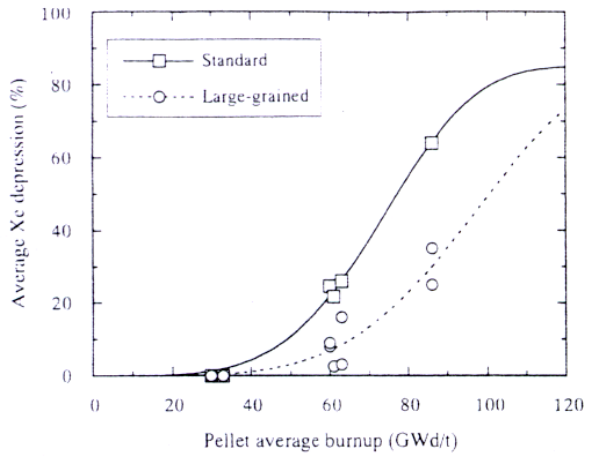

Fig. 7. Burnup dependence of average Xe depression in pellet outside region for fuel pellets irradiated in IFA551 and IFA566 rigs [16].

Burnup dependence of the average Xe depression in pellet outside region for pellets irradiated in IFA551 and IFA566 rigs are summarised in Fig. 7. With increasing grain size, rim structure development rate is suppressed, and the Xe depressions at 86 GWd/t for the large-grained pellets are about half of the value for the standard grain size pellet. This suggests that pellet size influence the rim structure formation.

Figs 5, 6 and 7 describe the same process of rim structure formation in function of burn-up. However, the difference is that once the process is described in terms of xenon concentration change with burn-up and once the process is described in terms of xenon depression change with burn-up. It is obvious from these figures, that the big scatter of the xenon concentrations in fig. 5 after crossing the first threshold burn-up is caused by different grain sized fuel from different reactors.

A very important structure remark of the UO_2 fuel is the decrease of the fuel lattice constant in the 'athermal' rim region. This can be indirectly appreciated [17] in Fig. 8 , where all available data of LWR-fuel lattice constants for T<800^o C, also for fuels with low and medium average burn-ups, are plotted versus local burn-up.

The figure shows in a first step a progressive lattice expansion in the range 0 –70 GWd/tM, attributable to the chemical reaction of fission gas products with the UO_2 fuel. A threshold burn-up above 70 GWD/tU occurs above which an abrupt lattice contraction takes place.

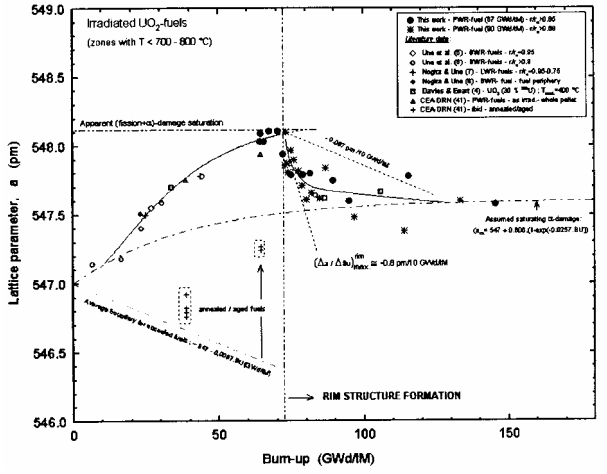

Fig. 8. Lattice parameter of irradiated fuels versus local burn-up (T<800^o C) [17].

This that the fuel lattice constant in the ‘athermal’ rim region increases linearly versus local burn up at the beginning and at the burn-up above about 50 GWd/tU the slope of the curve decreases can be explained by assumption that probability of rejection the oxygen from the crystal lattice and replacement by fission gas atoms is far bigger than the rejection probability of uranium. Replacement of oxygen by the fission gas atom causes enlargement of unit cell dimensions but in the case of uranium it is reversely. While the burn-up increases the amount of uranium vacancies increases due to fission and the probability of occupying the uranium vacancy by Kr and Xe increases also what explains the slope decrease of the curve which could be by intuition called mistakenly a saturation.

The linear increase of local xenon concentration as a function of the local burn-up in Figs 5 and 6 suggests the linear lattice constant expansion.

It seems to be natural that the chemically bound fission gas atoms substituting for example uranium atoms in the crystallographic lattice can form weak facets. At certain saturation conditions subdivision of the grains can occur what in turn cause the increase of total surface area and the increase in fission gas products release may be expected.

Considering the formation of the weak facets in crystallographic lattice of the grain due to substitution by the fission gas atom of the uranium atom, we have to keep in mind that the grain consists of a huge number of atoms. Some of the gas atoms can become noble gas atom again, stop to be chemically bound with the UO_2 fuel, electrical neutrality is restored and in consequence their chemical inertness is restored. Due to an “electrical spike” created by fission fragment the fission gas products bound chemically with the UO_2, can restore their closed shell electronic structure. Being located further in the same point defects the noble again fission gas products create weak sites in the uranium dioxide matrix.

The higher is the concentration of gas atoms immobilized in the uranium dioxide matrix, the more are the weak crystallographic sites. Crossing the threshold gas atom concentration, the weak sites can form new grain boundaries.

Keeping in mind that the fission gas release from the UO_2 grains during polygonization is athermal [14, 18] we infer that the knock-out release process is a significant process. This concept is consistent with this that TEM examinations of fully transformed material anticipate still large amount of gas within the restructured grains [17]. Still plenty of gas bubbles are observed within the small grains (150 nm – 300 nm), with more abundant precipitation these bubbles at the grain interiors, than on grain boundaries. These features can remain at burn-ups far beyond the rim-transformation threshold (e.g. at > 80 MWd/kgU) [17].

Sub-grain size histograms were constructed for various depth into fuel. Examples of these from 50 μm depth to 1570 μm are shown in Fig. 8 a – e [19].

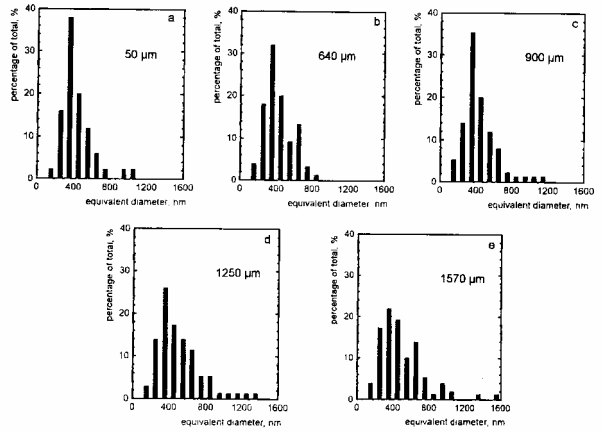

Fig. 8. Sub-grain size histograms for various depth from fuel surface [19].

At 1700 μm the nanostructure was no longer found at all. This thus can be taken to represent the limit for this particular fuel.

It is interesting to note that the grain size histograms do not vary significantly with depth into the fuel, and always show a peak between 300 nm and 400 nm. This means that the grain of diameter 6 μm can be divided into about 3000 and 8000 sub-grains.

The main variation with depth is the decreasing proportion of regions showing this structure as opposed to the normal grain structure of the fuel, from 100 % at the very rim to a very small proportion at depth> 1 mm. At a depth of 1.6 to 1.65 mm from the fuel surface grain subdivision occur only apparently at very few preferential sites, at grain boundaries or within pores.

The mechanism leading to the to the formation of this microstructure (grain subdivision or polygonization) is not fully satisfactorily understood at the present time [19].

For very high burn-up the process of grain sub-division (polygonization) occurs under condition that the temperature of irradiated fuel lies below the temperature of re-crystallization.

This is concluded from the experimental data showing that the re-crystallized grain region is found to be adjacent to the sub-divided grain region [20.]

Assuming that the Vitanza curve [21] describes the change of uranium dioxide re-crystallization temperature it was inferred that the grain growth rate depends on the burn-up in the way given by the best fit of the grain size change with the curve [22]. This enabled to modify the Ainscough's grain growth model and to infer that the higher is the initial grain size, the higher is the threshold temperature of re-crystallization of the grain. It means, if the limiting grain size for the appointed temperature is equal to the initial grain size, then the re-crystallization does not occur and in consequence, the polygonization process can begin if the threshold burn-up is crossed.

For example for the initial grain size of 5 μm the high burn-up nanostructure may be formed up to a temperature as high as 1000 ^{o}C, while for the initial grain size of 8 μm the nanostructure can be formed to a temperature as high as 1350 ^{o}C.

It is hoped that the above experimental analysis gives a reliable base to make a mathematical construct that will explain consistently the observed phenomena without any artificial assumptions.

3.1. Xenon concentration in rim layer of the grain subdivided fuel.

Knowing the temperature distribution in the fuel rod and the initial grain size we can evaluate how far the nanostructure zone may extend into the UO_2 pellet when the threshold burn-up is approached.

Simultaneously with the process of polygonization, the increase in local porosity and the decrease in local density in function of burn-up occurs, which leads to the increase of total surface area.

Keeping in mind that the fission gas release from the UO_2 grains during polygonization is athermal we infer that the knock-out release process is a significant process.

If some gas is trapped in the bubbles and it is experimentally proved that the formed gas bubbles are destroyed by the fission fragments, then some gas atoms have to be immobilized in the crystallographic lattice as gas atoms chemically bound with the fuel. So the same processes take place in the transformed fuel as in the original fuel, with the difference that the total surface area is so big that the whole fuel can be treated as that affected by the knock-out process described in the defect trap model.

For the steady state and for a step function of the fission rate, the solution of the defect

trap model equations, gives the following expressions for the concentration (N_{tr}) of bubbles, the concentration ($M._{tr}$) of gas atoms trapped in the bubbles and the concentration (M_r) of gas atoms immobilized in the lattice:

$$N_{tr} = \frac{g_1}{g_2 + g_3} \tag{4}$$

$$M_{tr} = \frac{\beta_i}{g_2} \tag{5}$$

$$M_r = \frac{\beta_i}{\alpha_1\left[\left(\frac{1}{\alpha_2} - \frac{g_3 g N_{tr}}{\alpha_2(g_2 + g_3)}\right) - 1\right]} \tag{6}$$

Where g, g_1, g_2, g_3, α_1, α_2, - constants

The gas atoms will not be accumulated as that in the bulk of the fuel but reach certain saturation level since the fission gas release rate will be equal the production rate according to the defect trap model:

$$g_2 f M_{tr} = \beta_i f \tag{7}$$

So we obtain that the concentration of gas atom trapped in the bubbles is equal as that in the equation (5) obtained in the result of solution of the defect trap model equations for stable state and the step function of fission rate. This is in agreement with the experimental data that for very high burnup (>120 MWd/kgU) the concentration of xenon is constant.

To calculate the concentration of retained Xe for the stable state when the equilibrium between the generated and released Xe is approached, the following appropriate values for the constants were used: $\alpha_1 = 10^{-19}$ cm^3, g = 10^{-18} s^{-1}, g_1 = 10, $g_2 = 10^{-15}$ cm^3, $g_3 = 10^{-17}$ cm^3. Some comments on the estimation of the constant parameters were presented previously. The xenon fission yield is approximated by 0.268.

With this values of constants, using the Eq. (5) and Eq. (6) we calculated that the xenon concentration is 2,67 10^{20} atoms/cm^3 what corresponds to about 0.5 wt % of Xe concentration. This theoretical result is very close to the experimental result of 0.25 wt % given by Lassmann et al [14].

3.2. Total surface area in the “athermal” rim region.

In the defect trap model the fission gas release (R) is described:

$$R = g_2 f M_{tr} \frac{(Sxr)}{V} \tag{8}$$

where S – total surface area, r – average fission fragment range, V – volume of the subdivided fuel.

When S x r is equal V then total surface area stops to increase. It means that the process of poligonization is ended.

Considering one cubic centimeter of subdivided fuel and assuming that r = 6 μm we obtain that total surface is equal to about 1.6 10^3 cm^2/cm^3. Relative density of the fuel for this total surface area is equal to about 89 % from figure 1. So the porosity is equal to about 11 %.

Comparing the result of porosity (11%) with the porosity given in reference [17] we see quite good agreement (15 %). So, in turn, we obtain the value of total surface area equal to about 9 10^3 cm^2/cm^3 for 85 % relative density, which we can call the limiting total surface area (S_l).

We can further assume the Gauss type distribution of grain size in the UO_2 fuel. This means that first and foremost the smaller grains start to subdivide. From experimental data we infer that the smaller is the grain the smaller is the saturation concentration of fission gas in the grain at which the subdivision begins.

This analysis let us to postulate that the total surface area of the subdivided fuel in the rim region is:

$$S = S_{bp} + (S_l - S_{bp})(1 - e^{-cb}) \tag{9}$$

where c is a constant dependent on the grain size, b – burn-up, S_{bp} – total surface area before the polygonization described by the equation 3.

4. Conclusions

Inter-linkage process of the fuel porosity starts to increase at about fuel burn-up equal to 12 MWd/kgUO_2 and becomes stabilized at about 30 MWd/kgUO_2 what causes the increase of total surface area and in consequence causes increase of fission gas release.

Above the limiting value of fission fluency a significant part of fission gas products are chemically bound in the UO_2 matrix. At certain saturation conditions (at burn-up equal to about 75 MWd/kgUO_2) the chemically bound fission gas atoms substituting for example the uranium atoms can restore their closed “shell electronic” structure due to “the electrical spike” created by fission fragments and in consequence can form weak facets where the subdivision can take place.

The process of grain growth and the process of grain subdivision are the processes of purging the contaminated lattice to some extent.

The same processes exist in the subdivided fuel as in the original fuel, with the difference that the total surface area is so big that the whole fuel can be treated as that affected by the knock-out process described in the defect trap model.

The subdivision of grains continues as long as the total surface area of the sample reaches the value when the restructured fuel is affected exclusively by the knock-out process.

The gas atoms in the subdivided fuel are not accumulated as that in the bulk of the fuel but reach certain saturation level since the fission gas release rate is equal the production rate.

The calculated and the experimental results of fission gas concentration in the fuel after polygonization are very close, and therefore give us confidence in the concept of the interpretation presented in this paper.

Correlation of the threshold burn-up, the local fission gas concentration, local total surface area, initial and local grain size and burn-up in the rim region is expected.

It is hoped that the above experimental analysis gives a reliable base to make a mathematical construct that will explain consistently the observed phenomena without any artificial assumptions.

References

[1] B. Lustman; Irradiation effects in uranium dioxide; Atomizdat, Moscow 1964.

[2] J. D. Eichenberg, P.W. Frank, T.J. Kisiel, B. Lustman and K.H. Vogel; Effects of irradiation on Bulk uranium Dioxide. In: Fuel Elements Conference, Paris. TID-7546, March, pp. 616-717.

[3] S. Aronson, J. C. Clayton, J. Rulli, T. R. Padden; Surface Areas of Sintered UO_2 Compacts. AECL-692. Aug. 1958.

[4] Y. Osawa, Fission gas release from nuclear fuels, (II); Fission gas release from nuclear fuels during low temperature, low dose irradiation., *J Nucl. Scien. and Techn*., 2,[8] (1965)296.

[5] R. M. Cornell, An Electron Microscope Examination of Matrix Fission-Gas Bubbles in Irradiated Uranium Dioxide, J. Nucl. Mater. 38 (1971) 319-328.

[6] M. Szuta, Fission gas release from UO_2 fuel during low temperature irradiation, *J. Nucl. Mater*. 58(1975)278-284.

[7] R. S. Nelson, J. Nucl. Mater. 31(1969)153.

[8] R. M. Carroll, O. Sisman, In-pile fission gas release from single crystal UO_2, *J Nucl. Sci. Eng*. 21(1965)147-158.

[9] K. Inoue, K. Taniguchi, Y. Ohsawa, Recoil Release of fission gas from UO_2*; J. Nucl. Sci. Technol*. 4(8) (1967)387-393.

[10] R. M. Carroll, O. Sisman „ Fission gas release during fissioning in UO_2" *Nucl. Application* Vol. 2 April 1966.

[11 R. Soulhier, Fission gas release from UO_2 during irradiation up to 2000 ^oC, *Nucl. Appl*. 2(2)(1966)1138-141.

[12] J. A. Turnbull, C. A. Frisknay, J. R. Findlay, F. A. Johnson, A. .J. Walter, *J. Nucl. Mater*. 107 (1-982)168.

[13] P.A. Tempest, A. Haaland, E. Skattum; FissionProduct Release and Thermal Behaviour in the Gas Flow Rig IFA-504 upto 35 MWd/kgUO_2, Report HWR-248, OECD Halden Reactor Project, January 1990.

[14] K. Lassmann, C. T. Walker, J. Van de Laar, F. Linstrom, *J. Nucl. Mater*. 226(1995) 1.

[15] M. Mogensen, J.H. Pearce, C.T. Walker, *J. Nucl. Mater*. 264(1999) 99-112

[16] K. Une, M. Hirai, K. Nogita, T. Hosokawa, Y. Suzawa, S. Shimizu, Y. Etoh*; J. Nucl. Mater*. 278(2000) 54.

[17] D. Baron, J. Spino. D Papaioannou, I Ray*; Seminar proceedings on "Fission Gas Behaviour in Water Reactor Fuels"* Cadarache, France, 26-29 September 2000, p247-268.

[18] Hj. Matzke, H. Blank, M. Coquerelle, K. Lassmann, I.L.F. Ray, C. Ronchi and C.T. Walker, *J. Nucl. Mater.* 166, (1989) 165.

[19] I.L.F. Ray, Hj. Matzke, H.A. Thiele, M. Kinoshita; *J. Nucl. Mater*. 245(1997) 115-123.

[20] K. Nogita, K. Une; Radiation-induced microstructure change in high burnup UO_2 fuel pellets; Nucl. Instr. And Meth. In Physics Reser. B91(1994) 301-306.

[21] C. Vitanza, E. Kolstad, U. Gracini; Proc. Am. Nucl. Soc., Topical Meeting on Light Water Reactors Fuel Performance, American Nuclear Society, Portland (OR) 1979, p.361.

[22] M. Szuta, M.S. El-Koliel; Modification of recrystallization temperature of uranium dioxide in function of burn-up and its impact on fission gas release; Acta Physica polonica A Vol. 96 (1999)143-151.